*Epilepsia*, 53(11):1959–1967, 2012
doi: 10.1111/j.1528-1167.2012.03675.x

FULL-LENGTH ORIGINAL RESEARCH

# Loss of $\beta_1$ accessory $Na^+$ channel subunits causes failure of carbamazepine, but not of lacosamide, in blocking high-frequency firing via differential effects on persistent $Na^+$ currents

***Mischa Uebachs, *Christina Albus, *Thoralf Opitz, †Lori Isom, ‡Isabelle Niespodziany, ‡Christian Wolff, and *Heinz Beck**

***Department of Epileptology, University of Bonn, Bonn, Germany; †Department of Pharmacology, University of Michigan, Ann Arbor, Michigan, U.S.A.; and ‡UCB Pharma, Braine l'Alleud, Belgium**

## Summary

**Purpose: In chronic epilepsy, a substantial proportion of up to 30% of patients remain refractory to antiepileptic drugs (AEDs). An understanding of the mechanisms of pharmacoresistance requires precise knowledge of how AEDs interact with their targets. Many commonly used AEDs act on the transient and/or the persistent components of the voltage-gated $Na^+$ current ($I_{NaT}$ and $I_{NaP}$, respectively). Lacosamide (LCM) is a novel AED with a unique mode of action in that it selectively enhances slow inactivation of fast transient $Na^+$ channels. Given that functional loss of accessory $Na^+$ channel subunits is a feature of a number of neurologic disorders, including epilepsy, we examined the effects of LCM versus carbamazepine (CBZ) on the persistent $Na^+$ current ($I_{NaP}$), in the presence and absence of accessory subunits within the channel complex.**

**Methods: Using patch-clamp recordings in intact hippocampal CA1 neurons of *Scn1b* null mice, $I_{NaP}$ was recorded using slow voltage ramps. Application of 100 μM CBZ or 300 μM LCM reduced the maximal $I_{NaP}$ conductance in both wild-type and control mice.**

**Key Findings: As shown previously by our group in *Scn1b* null mice, CBZ induced a paradoxical increase of $I_{NaP}$ conductance in the subthreshold voltage range, resulting in an ineffective block of repetitive firing in *Scn1b* null neurons. In contrast, LCM did not exhibit such a paradoxical increase, and accordingly maintained efficacy in blocking repetitive firing in *Scn1b* null mice.**

**Significance: These results suggest that the novel anticonvulsant LCM maintains activity in the presence of impaired $Na^+$ channel $\beta_1$ subunit expression and thus may offer an improved efficacy profile compared with CBZ in diseases associated with an impaired expression of β subunits as observed in epilepsy.**

**KEY WORDS: Carbamazepine, Lacosamide, Sodium channel beta subunits, $\beta_1$ Subunit, Persistent sodium current, $I_{NaP}$, Epilepsy.**

Lacosamide (LCM, SPM927) is a new antiepileptic drug that recently received approval in the United States and Europe as add-on treatment for partial onset seizures (Cross & Curran, 2009). LCM has been shown to be efficient in rodent models of focal and generalized epilepsy, such as audiogenic seizures, maximal electric shock (MES)-induced seizures (Andurkar et al., 1999; Stöhr et al., 2007), and limbic seizures in the 6-Hz psychomotor seizure model (Stöhr et al., 2007; Duncan & Kohn, 2005). In addition, LCM is efficacious in limiting the generation of seizures and afterdischarges in the kindling model of epilepsy (Stöhr et al., 2007; Brandt et al., 2006). Finally, LCM potently blocks seizure activity elicited in vitro with the $K^+$ channel blocker 4-aminopyridine (Lees et al., 2006).

The precise mechanism by which LCM exerts its antiepileptic effect in animal models or humans remains to be fully elucidated. The preclinical observations that may be of relevance for the observed therapeutic effects are based on in vitro electrophysiologic studies demonstrating that LCM selectively enhances slow inactivation of voltage-gated fast transient sodium currents ($I_{NaT}$, Errington et al., 2008; Sheets et al., 2008). This novel mechanism of action was proposed to contribute to the anticonvulsant activity of LCM by preferentially rendering $Na^+$ channels less available during the high-frequency firing and depolarization shifts encountered during epileptiform activity. It is even more pronounced in derivatives of LCM (Wang et al., 2011), but the preclinical efficacy of these compounds is still unclear.

Accepted July 31, 2012; Early View publication September 27, 2012.
Address correspondence to Heinz Beck, Laboratory of Experimental Epileptology, Department of Epileptology, University of Bonn, Sigmund-Freud-Str. 25, 53105 Bonn, Germany. E-mail: heinz.beck@ukb.uni-bonn.de

Wiley Periodicals, Inc.
© 2012 International League Against Epilepsy

Neuronal excitability is not only critically determined by the properties of $I_{NaT}$. A noninactivating, low-voltage activated $Na^+$ current component, termed persistent $Na^+$ current ($I_{NaP}$), strongly contributes to neuronal excitability in the subthreshold range (Vervaeke et al., 2006; Yue et al., 2005). $I_{NaP}$ is a target for numerous AEDs with activity on $I_{NaT}$ (Sun et al., 2007; Taverna et al., 1998). A recent study has shown that the molecular composition of the $Na^+$ channel complex can affect anticonvulsant activity on $I_{NaP}$ (Uebachs et al., 2010). Specifically, the action of the anticonvulsant carbamazepine (CBZ) on $Na^+$ channel $I_{NaP}$ appears to depend on the presence of the accessory $\beta_1$ $Na^+$ channel subunit or its splice variant $\beta_1$B (also described as $\beta_1$A, Kazen-Gillespie et al., 2000). Surprisingly, CBZ induced a pronounced shift of the voltage-dependence of activation of $I_{NaP}$ to more hyperpolarized potentials in *Scn1b* null mice that lack functional $\beta_1$ subunits. This phenomenon led to a pronounced increase of $I_{NaP}$ within the subthreshold potential range, in particular at low CBZ concentrations of 10–30 $\mu$M. Intriguingly, this paradoxical enhancement of $I_{NaP}$ leads to a complete loss of CBZ efficacy in reducing repetitive action potential firing in *Scn1b* null mice. Consequently, altered expression of *Scn1b* in other neurologic disorders, or potentially human mutations in the *Scn1b* gene (Meadows et al., 2002; Wallace et al., 1998) may cause altered neuronal sensitivity to drugs targeting $Na^+$ channels. Because LCM has a mechanism of action that is distinct from other $Na^+$ channel acting compounds, we assessed whether LCM activity on $I_{NaP}$ and neuronal excitability is similarly affected by loss of accessory $\beta_1$ subunits. Our results indicate that LCM activity—in contrast to CBZ—is preserved in the absence of *Scn1b*, suggesting a rationale for an improved clinical profile in neurologic disorders with loss of these subunits. However, to establish the clinical utility of LCM in pharmacoresistance mechanisms related to *Scn1b*, further data from a relevant disease model or from a clinical study are needed.

## Methods

### *Scn1b* null mice

The generation of *Scn1b* null mice has been described previously (Chen et al., 2004). Animals used in this study were bred from congenic *Scn1b*$^{+/-}$ mice of generation N10 or higher bred on the C57BL/6 genetic background. Experiments were performed on slices or dissociated neurons from the hippocampus of male *Scn1b* null mice and their wild-type littermates. Animals were used between postnatal days P12–20 because *Scn1b* null mice die at approximately P20 (Chen et al., 2004). It is important to note that these animals lack both $\beta_1$ as well as the splice variant $\beta_1$B (also termed $\beta_1$A, Kazen-Gillespie et al., 2000). All animal experiments were performed in accordance with the regulations of the local animal care and use committee.

### Slice preparation

Animals were decapitated under ether anesthesia, and transverse hippocampal slices (300 or 400 $\mu$m) were prepared with a vibrating microslicer (Leica VT 1000 S; Leica, Wetzlar, Germany) and transferred to a storage chamber perfused with oxygenated (5% $CO_2$ – 95% $O_2$) artificial cerebrospinal fluid (ACSF) containing (in mM): NaCl 125, $NaHCO_3^-$ 25, KCl 3.5, $NaH_2PO_4$ 1.25, $MgCl_2$ 1, $CaCl_2$ 2, glucose 25, pH 7.4.

### Preparation of isolated neurons

Dissociated hippocampal neurons were prepared as described previously (Schaub et al., 2007). After an equilibration period (>60 min), enzymatic digestion was carried out for 10 min at 37°C and 5 min at room temperature in 5 ml of incubation medium containing (in mM): Sodium methanesulfonate (NaMS) 145, KCl 3, $CaCl_2$ 0.5, $MgCl_2$ 1, N-2-hydroxyethylpiperazine-N-2-ethanesulfonic acid (HEPES) 10, glucose 15, and pronase (protease type XIV; Sigma, Taufkirchen, Germany) 2 mg/ml (pH 7.4, osmolarity 310 mOsmol, 100% $O_2$). After washing with enzyme-free incubation medium, the CA1 region was dissected and triturated with fire-polished glass pipettes. The cell suspension was placed in a petri dish.

### Patch-clamp recording

For patch-clamp recordings, slices or dissociated cells were continuously perfused with an extracellular solution containing (in mM): $CH_3SO_3Na$ 100, TEA-Cl 40, $CaCl_2$ 2, $MgCl_2$ 3, HEPES 10, 4-aminopyridine 5, $CdCl_2$ 0.2, and glucose 25, pH 7.4 adjusted with NaOH, osmolality 315 mOsm, 21–24°C. Pyramidal cells in the CA1 field were visualized at 600× magnification with DIC optics using a Nikon FN-1 microscope (Nikon, Tokyo, Japan) and an infrared video camera for recordings from slices. The petri dish with the isolated cells was mounted on an Axiovert100 microscope (Zeiss, Oberkochen, Germany), and pyramidal cells were identified by their morphology. Patch pipettes (3–5 MΩ) were pulled from borosilicate glass on a vertical puller (Narishige, Japan). They were filled with intracellular solution containing (in mM): CsF 110, HEPES-Na 10, ethylene glycol-bis(2-aminoethyl-ether)-N,N,N′,N′-tetraacetic acid (EGTA) 11, $MgCl_2$ 2, TEA-Cl 20, GTP-Tris 0.5, ATP-$Na_2$ 5, pH 7.2. Whole cell patch-clamp recordings were obtained using an Axopatch 200B amplifier and pClamp 10.0 software (Molecular Devices, Sunnyvale, CA, U.S.A.) or an EPC9 amplifier and PATCHMASTER software (HEKA, Elektronik, Lambrecht, Germany) for recordings from slices or isolated neurons, respectively. For all voltage-clamp experiments, all voltages were corrected for a liquid junction potential of −10 mV. Without correction potentials would be 10 mV more negative. The series resistance was <15 MΩ, and was compensated 50–80%, resulting in a voltage error <3 mV for all measurements.

### Sharp microelectrode recordings

For intracellular sharp microelectrode recordings, 400-$\mu$m thick hippocampal slices were placed in an interface chamber (35 ± 1°C) and perfused with oxygenated artificial cerebrospinal fluid (ACSF) containing (in mM): NaCl 125, KCl 3.5, $NaH_2PO_4$ 1.25, $MgCl_2$ 2, $CaCl_2$ 2, $NaHCO_3$ 26, and D-glucose 15. Intracellular recordings were obtained using sharp glass microelectrodes containing 3 M $K^+$-acetate (90–110 MΩ). An active bridge circuit in the amplifier (Axoclamp 2B; Molecular Devices) allowed simultaneous injection of current and measurement of membrane potential. After stabilization of neurons, the compound was applied by adding it to the ACSF. The effects reached a plateau 15 min after wash-in and were evaluated 20 min after wash-in. Bridge balance was carefully adjusted before each measurement and experiments were discarded if it changed by >10%. The signals were filtered on-line at 10 kHz, digitized at a sampling rate of 100 kHz, and stored on hard disk (pClamp 8; Molecular Devices).

### Solutions

LCM and CBZ were prepared in stock of 300 and 100 mM, respectively, in ethanol and added to the bath 1:1,000. Control ACSF included equal concentrations of ethanol. We applied concentrations of 30–1,000 and 30–300 $\mu$M in the experiments on $I_{NaP}$ and the action potential firing behavior, respectively. This covers a wide range of reported free serum concentrations (reviewed in Kellinghaus, 2009) and resembling other studies describing the mode of action (Errington et al., 2008), albeit one recent study reports a relatively high protein binding that would result in much lower free serum concentrations (Greenaway et al., 2011).

### Voltage clamp paradigms and data analysis

Slow voltage ramps (50 mV/s from a holding potential of −80 to +30 mV, see uppermost trace in Fig. 3A) were applied to elicit $I_{NaP}$ without recruiting fast transient $Na^+$ currents ($I_{NaT}$) and a current trace obtained during application of Tetrodotoxin (TTX, 0.5 $\mu$M) was subtracted from each recording to pharmacologically isolate the $Na^+$ mediated currents. The conductance G(V) was calculated according to

$$G(V) = I(V)/(V - V_{Na})$$

where $V_{Na}$ is the $Na^+$ reversal potential, V the ramp potential, and I(V) is the recorded current. G(V) then was fitted for each family of traces obtained from individual cells with the following Boltzmann equation:

$$G(V) = A_1 + \frac{(A_0 - A_1)}{(1 + e^{(V - V1/2)/k})}$$

where $A_0$ and $A_1$ are $Na^+$ conductances, $V_{1/2}$ is the voltage where G(V) is half of maximal conductance, and k indicates the slope of the relation between channel activation or inactivation and membrane voltage. Because a time-dependent leftward shift of $V_{1/2}$ was described previously in patch-clamp recordings, we corrected the values for this shift to isolate the drug-induced effects (Uebachs et al., 2010). A nonlinear Levenberg-Marquardt algorithm was used for all fits. In all cases, fits were performed on the data points obtained from individual cells; these parameters were then averaged. All results are presented as the mean ± standard error of mean.

### Current clamp data analysis

The voltage traces recorded in current clamp mode with sharp microelectrodes were analyzed with Igor Pro (Wavemetrics, Lake Oswego, OR, U.S.A.). Action potentials were described quantitatively by determining their peak amplitude, the maximal rate of rise of the voltage trace, and the action potential threshold. The action potential threshold was determined as the voltage at which the slope of the voltage trace exceeded 15 mV/msec (Sekerli et al., 2004). Repetitive firing was examined using prolonged current injections (500 msec). Input–output relations were obtained with an automatic action potential detection routine programmed in Igor Pro. To assess the effects on the subthreshold depolarization we used defined current injections set to a value of 2× the threshold current injection. We determined the slope of the interspike interval as the average of the first derivative of the voltage trace within the interspike interval from the most hyperpolarized point to the spike threshold. For this analysis, we chose the interspike interval preceding the first action potential detected beginning 100 msec after the start of the recording. This interspike interval was selected to ensure that passive charging of the membrane capacitance had completed for all cells in order to avoid contamination of the interspike slope.

### Statistical analyses

Statistical comparison was performed with a Student's *t*-test at a significance level $\alpha$ of 0.05. When appropriate, paired tests were used to compare the recordings before and during application of 100 $\mu$M CBZ or 300 $\mu$M LCM. Unpaired tests were used for group comparisons of null mice to their wild-type littermates regarding channel properties and drug effects. Two way analysis of variance (ANOVA) was used to compare the input–output gain before and following application of drugs. The results of the statistical analysis are given throughout the results section and figure legends and significance levels $p < 0.05$ are indicated in the figures with asterisks.

## Results

### Effects of LCM and CBZ on repetitive neuronal firing

We first examined the effects of LCM and CBZ on high-frequency action potential firing of CA1 neurons. We used sharp microelectrode recordings, as they are well-suited for

long-term stable recording of discharge properties and prevent washout of cytosolic proteins (Xu et al., 2005; Müller et al., 2007). We obtained sharp microelectrode recordings from CA1 pyramidal neurons in acute slices and elicited repetitive action potential firing with depolarizing current injections (Fig. 1A–D; representative traces for a current injection of 500 pA under control conditions and after drug application are shown in the upper part of the panels in black and green, respectively). Increasing the magnitude of the current injection (0–600 pA) allowed us to generate input–output gain curves, with larger current injections causing a higher average action potential frequency. In *Scn1b* wild-type mice, application of either CBZ (100 $\mu$M) or LCM (300 $\mu$M) potently and significantly blocks repetitive firing, thereby reducing input–output gain (Fig. 1A,C, compare black and green symbols, $p < 0.05$ two-way ANOVA, n = 7 and 7, respectively). This reduction of high-frequency repetitive discharges is thought to underlie the specific effects of many $Na^+$ channel acting anticonvulsant drugs. We next examined the efficacy of CBZ and LCM in blocking repetitive firing in *Scn1b* null mice. As reported previously (Uebachs et al., 2010), genetic deletion of $\beta_1$ and/or $\beta_1$B subunits results in a complete loss of CBZ efficacy in blocking repetitive firing (Fig. 1B, n = 7). Because this loss of CBZ efficacy may be a candidate mechanism for the development of pharmacoresistance to this drug, we were interested in studying whether LCM, which presents a different mechanism of action on $I_{NaT}$, may overcome the effects of CBZ. We examined the effects of LCM in *Scn1b* null mice and found that loss of $\beta_1/\beta_1$B subunits does not affect sensitivity to LCM significantly (Fig. 1D, n = 5) within the range of LCM concentrations examined (30–300 $\mu$M, see Fig. 1E).

We then further explored why efficacy of LCM is maintained in this experimental paradigm. We first examined how the passive properties of the membrane and the properties of individual action potentials are affected. Both CBZ (100 $\mu$M) and LCM (300 $\mu$M) shifted the action potential threshold slightly in a depolarizing direction and reduced the slope of the action potential (see Table 1) probably due to the reduction of $I_{NaT}$ conductance. This effect was not dependent on the *Scn1b* expression and provides no explanation for the differential effect both substances exert on the repetitive firing behavior. As described previously

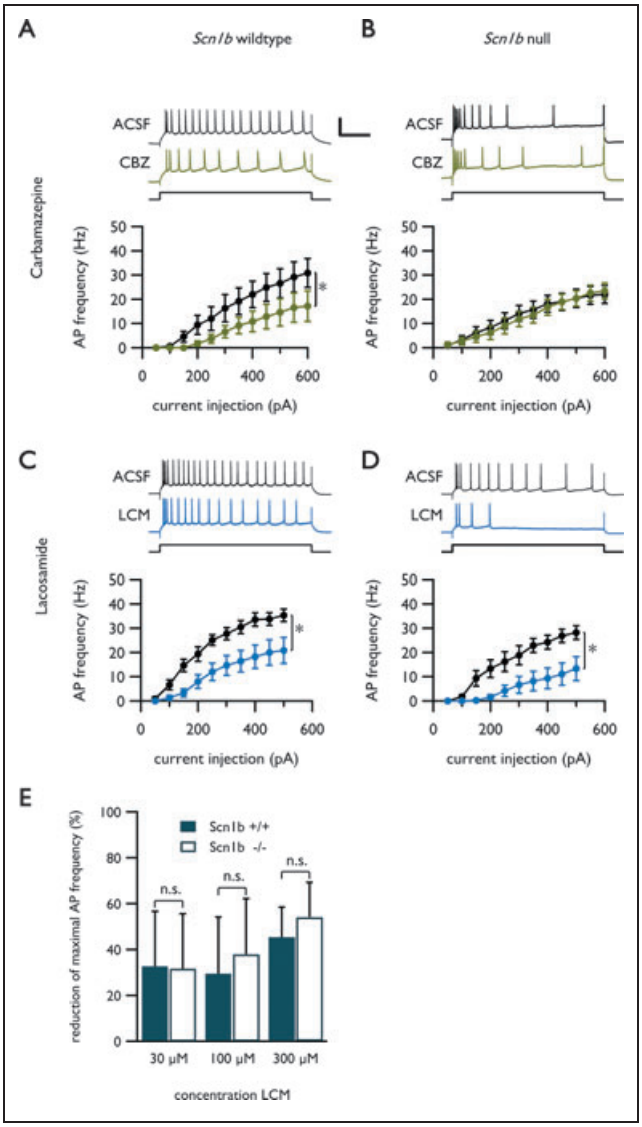


**Figure 1.**
Effects of carbamazepine and lacosamide on the input–output gain of pyramidal cells. Sharp electrode recordings of CA1 pyramidal neurons were obtained before (black traces in all panels) and during application of 100 $\mu$M CBZ (green traces in panels **A** and **B**) or 300 $\mu$M LCM (blue traces in panels **C** and **D**). Repetitive firing was elicited with prolonged current injections (500 msec) of varying magnitude (50–600 pA, representative traces for a current injection of 500 pA are shown in the upper part of each panel together with the corresponding current injection of 500 pA, scale bars in panel **A** correspond to 100 msec and 50 mV and apply for all panels). The frequency of the action potential train was depicted versus the amplitude of the current injection. (**A**) Application of 100 $\mu$M CBZ reduced the input–output gain significantly ($p < 0.05$, n = 7) in wild-type animals. (**B**) CBZ failed to reduce the frequency of repetitive firing in *Scn1b* null mice (n = 7). (**C**) LCM induced a similar reduction of firing frequency in wild-type mice ($p < 0.05$, n = 7). (**D**) This effect was maintained in mice lacking the $\beta_1$ subunit ($p < 0.05$, n = 5). *Significance level <0.05 in the paired two-way ANOVA for statistical comparison over the full range of current injections. (**E**) Lack of significant differences between the *Scn1b* null and wild-type mice with regard to the effects of different concentrations (30–100 $\mu$M) of LCM (n = 5). Maximal action potential frequency was determined for each individual cell under control conditions and following application of LCM.
*Epilepsia* © ILAE

**Table 1. Effects of CBZ and LCM on action potential parameters**

| | Threshold (mV) | Max. slope (mV/ms) | Amplitude (mV) | $R_m$ (MΩ) |
|---|---|---|---|---|
| Scn1b +/+ (7) | | | | |
| ACSF | −52.6 ± 2.2 | 161 ± 9 | 68.5 ± 3.4 | 52.7 ± 7.2 |
| CBZ | −48.2 ± 2.6* | 150 ± 11* | 64.3 ± 3.0* | 53.2 ± 12.7 |
| Scn1b −/− (8) | | | | |
| ACSF | −57.4 ± 2.6 | 159 ± 9 | 69.5 ± 2.7 | 68.2 ± 9.7 |
| CBZ | −50.2 ± 3.0* | 146 ± 5* | 68.0 ± 3.6 | 82.3 ± 12.7 |
| Scn1b +/+ (8) | | | | |
| ACSF | −56.2 ± 1.1 | 149 ± 5 | 64.3 ± 1.4 | 68.8 ± 10.8 |
| LCM | −52.7 ± 1.6* | 145 ± 5* | 62.6 ± 0.7 | 56.7 ± 12.9 |
| Scn1b −/− (5) | | | | |
| ACSF | −53.6 ± 1.0 | 145 ± 5 | 63.7 ± 1.7 | 60.0 ± 7.0 |
| LCM | −51.8 ± 1.0* | 138 ± 7* | 60.5 ± 1.9* | 38.4 ± 4.1* |

CBZ (100 μM) and LCM (300 μM) shift the action potential threshold in a depolarized direction and slightly reduce depolarization rate and amplitude of the action potential significantly. No significant difference of either parameters under control conditions or of the effects of the AEDs was found when comparing the *Scn1b* null mice to their wild-type littermates. Number of analyzed cells is given in brackets.

*Significant alterations of the parameters induced by the AED.

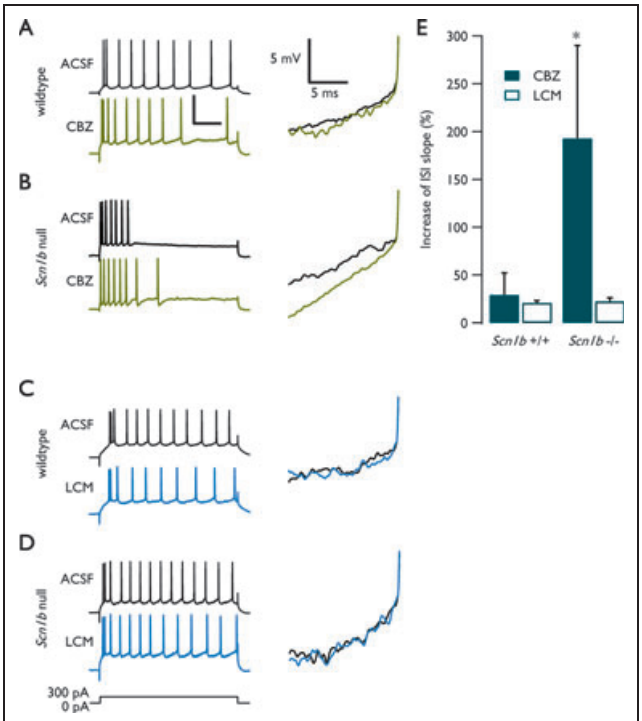


**Figure 2.**

Carbamazepine but not lacosamide accelerates the interspike depolarization in *Scn1b* null mice. (**A**, **B**) Closer analysis of the recordings described in Fig. 1 (leftmost traces, scale bars in panel **A** correspond to 100 msec and 50 mV and apply for all panels) revealed a steeper slope of the interspike depolarization when applying 100 μM CBZ in *Scn1b* null mice (green traces in panel **B**) but not in their wild-type littermates (green traces in panel **A**, the analyzed interspike interval is magnified and shifted to overlay the points of threshold for better comparison in the right part of panels **A**–**D**). (**C**, **D**) Application of 300 μM LCM did not affect the interspike depolarization both in wild-type (panel **C**) and *Scn1b* null mice (panel **D**). (**E**) The slope of the interspike depolarization was quantified as the average of the first derivative of the voltage trace for all cells and the average ± SEM depicted for CBZ (filled bars) and LCM (open bars) for both genotypes, displaying a significant increase of the interspike depolarization by CBZ in *Scn1b* null mice ($p < 0.05$).

*Epilepsia* © ILAE

(Uebachs et al., 2010), CBZ application in *Scn1b* null mice leads to a pronounced increase in the slope of interspike depolarization (Fig. 2B, rightmost traces), which was not seen in *Scn1b* wild-type mice (Fig. 2A, rightmost traces). This finding is important, because an increase in the rate of interspike depolarization would be expected to increase the firing rate, thereby counteracting other effects of CBZ that lower the firing rate (Uebachs et al., 2010). Indeed, the acceleration of interspike depolarization upon CBZ application was highly significant in *Snc1b* null mice (Fig. 2E, filled bars, see asterisk). When the same analysis was performed in *Scn1b* wild-type and null mice before and after application of 300 μM LCM, the rate of interspike depolarization was unaffected in both genotypes (Fig. 2C,D and open bars in Fig. 2E). This indicates a potential basis for the maintained efficacy of LCM on the firing rate of neurons in *Scn1b* null mice. No significant differences in the rate of the interspike depolarization under ACSF conditions were observed when comparing wild-type to *Scn1b null* mice.

### Effects of LCM on persistent $Na^+$ currents

The interspike depolarization is modulated by voltage gated ion channels that open within the subthreshold voltage range. In CA1 neurons, the main somatic subthreshold inward current is a persistent $Na^+$ current ($I_{NaP}$, Yue et al., 2005). Previous studies have established that CBZ can lead to paradoxical increases in $I_{NaP}$ in the absence of *Scn1b*, which induce an augmented speed of the interspike depolarization (see Uebachs et al., 2010; see also Fig. 2A,B). We now systematically examined the effect of LCM on $I_{NaP}$ in wild-type animals. Slow voltage ramps (50 mV/s from a holding potential of −80 mV, see uppermost trace in Fig. 3A) were applied to elicit $I_{NaP}$ without recruiting fast transient $Na^+$ currents ($I_{NaT}$). An inward current is observed when the depolarizing ramp reaches threshold voltage (Fig. 3A-a). This inward current is reduced following application of 300-μM LCM (Fig. 3A-b). To isolate $I_{NaP}$ pharmacologically, TTX (0.5 μM) was applied in all recordings, and the resulting current trace (Fig. 3A-c) was subtracted from traces in the absence of TTX. The resulting traces (Fig. 3B, a–c and b, c) represent $I_{NaP}$ under control conditions (a–c) and in the presence of LCM (b, c). The current traces were converted to conductance (see Methods) and depicted versus the voltage (Fig. 3C). Evidently, $I_{NaP}$ maximal conductance is reduced by application of LCM.

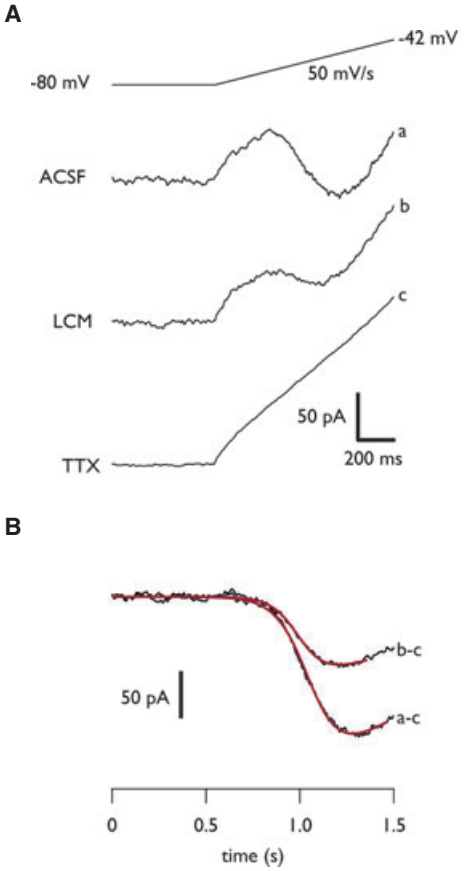


**Figure 3.**
Effects of lacosamide on $I_{NaP}$ in wild-type mice. (**A**, **B**) Voltage ramps (50 mV/s, uppermost trace in panel **A**) were applied to elicit $I_{NaP}$ before (trace a) and during application of LCM (trace b). Subsequently, TTX was applied (0.5 $\mu$M, trace c) and the resulting current trace subtracted from the other traces to isolate the $Na^+$ mediated current (panel **B**). The current traces were fitted by the product of a Boltzmann equation and the driving force that is linearly changing with time during the ramp (superimposed red lines in panel **B**). (**C**) The calculated conductance is depicted versus the ramp voltage, demonstrating the reduction of the maximal conductance induced by LCM. (**D**) The maximal conductance was significantly reduced in a concentration dependent manner (*$p < 0.05$, see brackets in panel **D** for number of recorded cells).
*Epilepsia* © ILAE

The reduction of the maximal $I_{NaP}$ conductance by LCM is concentration-dependent (Fig. 3D). Remarkably, the dose dependence was more pronounced for the effect on $I_{NaP}$ than observed for the effect on the frequency of repetitive action potential firing (compare Fig. 1E). A different dose response of the effects on one current component and on the resulting firing frequency is not surprising, since LCM is known to exert its effect not only on the $I_{NaP}$ but also on the $I_{NaT}$ (Errington et al., 2008; Sheets et al., 2008).

Next, we compared the effects of 300 $\mu$M LCM and 100 $\mu$M CBZ on the properties of $I_{NaP}$ in *Scn1b* null and wild-type mice. Both substances reduce the maximal $I_{NaP}$ conductance in *Scn1b* null mice as well as in their wild-type littermates (compare dashed lines to solid lines representing reconstructions of the voltage dependence of activation of representative cells in Fig. 4A,B,D,E). The $I_{NaP}$ conductance was reduced by approximately 50% in all groups, with no significant differences when comparing the effects in *Scn1b* null ($n = 6$ for both AEDs) versus wild-type mice ($n = 7$ and 5 for experiments with CBZ and LCM, respectively, Fig. 4G). However, CBZ induced a stronger hyperpolarizing shift of the voltage dependence of activation (Fig. 4B and open green bar in Fig. 4H) in *Scn1b* null mice than in *Scn1b* wild-type mice (Fig. 4A and filled green bar in Fig. 4H). LCM, on the other hand, did not affect voltage dependence of $I_{NaP}$ in either *Scn1b* null mice (Fig. 4E and rightmost bar in Fig. 4H) or in wild-type animals (Fig. 4D,H).

What are the consequences of differential LCM and CBZ effects on $I_{NaP}$? To assess how CBZ and LCM would affect inward current through $I_{NaP}$ in the subthreshold range, we quantified the maximum increase in $I_{NaP}$ caused by either CBZ or LCM. This maximum increase is indicated by the uppermost dashed line in Fig. 4C. As expected, CBZ did not cause a paradoxical increase in *Scn1b* wild-type mice (black line in Fig. 4C). However, CBZ caused a large paradoxical increase in $I_{NaP}$ conductance within the subthreshold range in *Scn1b* null mice (teal line in Fig. 4C). This increase amounted to $7.3 \pm 2.6\%$ of $g_{max}$ ($p < 0.05$, indicated by asterisks in Fig. 4I), and was not present in wild-type mice ($0.7 \pm 0.2\%$, n.s., Fig. 4I). The maximal paradoxical increase of $I_{NaP}$ is induced at $-55.4 \pm 0.4$ mV, which is within the interspike potential range (see Fig. 2A–D). In contrast to CBZ, LCM did not cause paradoxical increases in $I_{NaP}$ conductance in either wild-type or *Scn1b* null mice (Fig. 4F,I, rightmost bars).

## Discussion

The main finding of our study is that the novel anticonvulsant LCM strongly affects $I_{NaP}$. In contrast to the

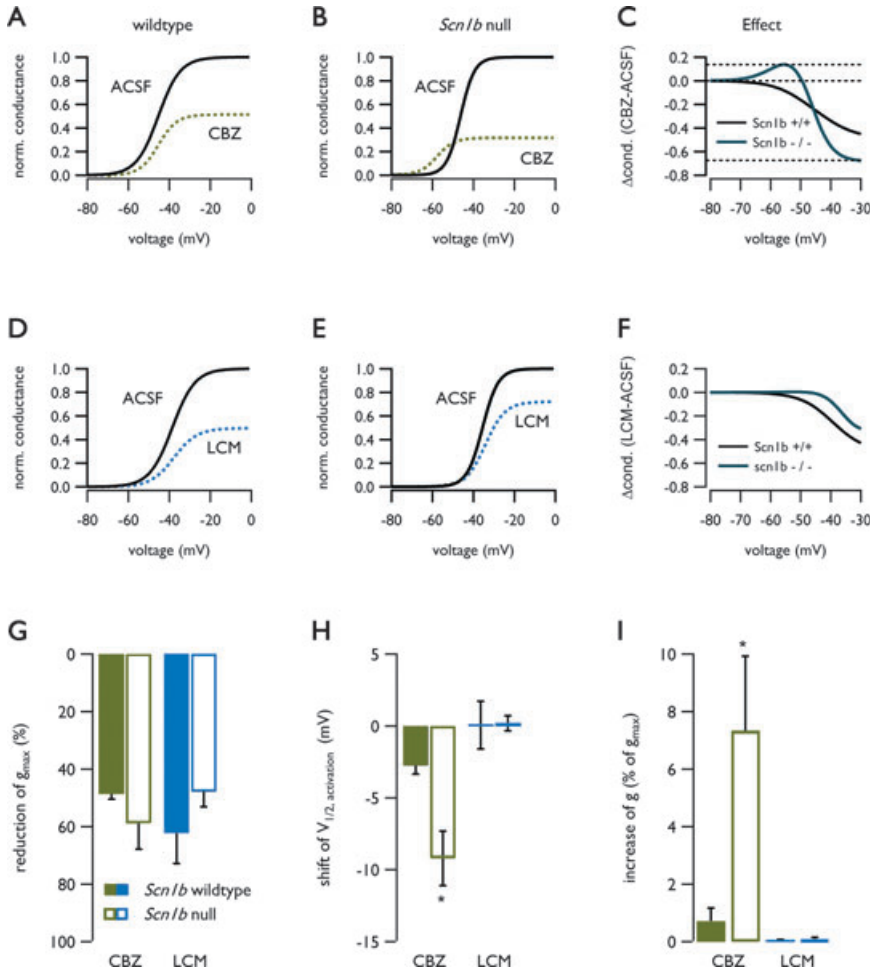


**Figure 4.**
Influence of the $\beta_1$ $Na^+$ channel subunit on the effects of CBZ and LCM. (**A**, **B**, **D**, **E**) Conductance voltage relation of $I_{NaP}$ was reconstructed with the parameters obtained from the Boltzmann fit of the recorded current traces and depicted for representative cells before and during application of 100 $\mu$M CBZ (panel **A** and **B**) or 300 $\mu$M LCM (panel **D** and **E**) in wild-type (panel **A** and **D**) and *Scn1b* null mice (panel **B** and **E**) demonstrating a pronounced left shift when applying CBZ to pyramidal cells from *Scn1b* null mice (panel **B**). (**C**, **F**) The effect of either CBZ (panel **C**) or LCM (panel **F**) was quantified as the difference between the normalized conductance before and during application of the substance (black and teal traces correspond to *Scn1b* wild-type and null mice, respectively). (**G**) The reduction of the maximal conductance, already apparent in panels **A**–**F**, did not depend on the presence of $\beta_1$ subunits (compare open to filled bars in panel **G**, n = 7 and 6 for the effects of CBZ in *Scn1b* wild-type and null mice and n = 5 and 6 for the effects of LCM in both groups, respectively). (**H**) The average of all recorded cells shows a significant CBZ induced left shift of the voltage of half maximal activation in *Scn1b* null (open green bar, see asterisk) but not in wild-type animals (filled green bar). LCM did not affect the voltage dependence of activation (rightmost bars). (**I**) Consequently an increase of $I_{NaP}$ conductance, quantified as percentage of the maximal conductance as indicated by the uppermost dashed line in panel **C**, was observed only for CBZ in *Scn1b* null mice (*significant increase of $I_{NaP}$ conductance induced by CBZ).
*Epilepsia* © ILAE

established anticonvulsant CBZ, for which effects on $I_{NaP}$ are strongly dependent on the presence of $\beta_1$ and/or $\beta_1$B subunits within the channel complex, this is not the case for LCM. In particular, CBZ was found to potently shift the voltage-dependence of activation of $I_{NaP}$ toward more hyperpolarized potentials in mice lacking *Scn1b*, leading to a paradoxical increase in $I_{NaP}$ in the subthreshold voltage range (see also Uebachs et al., 2010). In marked contrast, such an increase was not observed for LCM, even at a concentration of 300 $\mu$M. Consequently, the effects of LCM on neuronal firing were preserved in *Scn1b* null mice, in which CBZ was ineffective.

The expression of *Scn1b* is differentially regulated in animal models of neurologic disorders. In experimental

autoimmune encephalomyelitis (EAE), a model of multiple sclerosis, both *Scn1b* and *Scn2b* are transcriptionally downregulated (Nicot et al., 2003). Likewise, in some types of neurons, denervation appears to result in reduced expression of $\beta_1$ subunits (Sashihara et al., 1996). Finally, in models of chronic temporal lobe epilepsy both *Scn1b* and *Scn2b* mRNAs are down-regulated (Gastaldi et al., 1998; Ellerkmann et al., 2003). In addition, a recent article has shown that a functional null *Scn1b* mutation can result in a severe form of childhood epilepsy known as Dravet syndrome (Patino et al., 2009). These studies suggest that downregulation of $\beta_1$ subunits occurs in a number of neurologic disorders, or models thereof. Because our data suggest that loss of $\beta$ subunits affects the cellular CBZ response, but not the LCM response, it is tempting to speculate that the latter compound might be more efficacious under these conditions. However, it is by no means clear that a graded loss of beta subunits in disease models will have the same impact as the total loss of one of the beta subunits in our knockout mouse models. Direct confirmation of this hypothesis will therefore have to be obtained in models of central nervous system (CNS) disorders.

In addition, our results suggest that the biophysical mechanism of action of LCM on $Na^+$ channels is fundamentally distinct from that of the established anticonvulsant CBZ. Identification of the location of the receptor site for CBZ on the $Na^+$ channel has been attempted in a number of studies. CBZ appears to share a receptor site with other anticonvulsant drugs such as lamotrigine and phenytoin (Ragsdale et al., 1996; Kuo et al., 2000; Kellinghaus, 2009), but experiments aimed at a precise identification of the binding site have been difficult to merge into a unifying hypothesis (see comprehensive discussion in Yang et al., 2009). A recent study has resolved some of the extant controversy by proposing that the common drug-binding epitopes for CBZ, lamotrigine, and phenytoin involve structures in the external pore loop (W1716 in IVSS6), in the internal pore compartment of S6 in domain IV (F1764), as well as the S3-4 linker of domain 4. These three structures appear to interact intimately and to form the binding site for the main effects of CBZ on fast $Na^+$ channel physiology (Yang et al., 2009). However, whether these sites are also relevant for actions of CBZ on the persistent $Na^+$ current is unknown. A discussion of the reasons that LCM effects are insensitive to the presence of beta subunits, whereas the CBZ pharmacology is affected, is therefore speculative. The most straightforward explanation is that the binding site of LCM at the $Na^+$ channel $\alpha$ subunit is distinct from the CBZ binding site. This is indeed suggested by the diverse effects of the two compounds on transient $Na^+$ currents. Although CBZ exerts potent effects on fast $Na^+$ channel gating, LCM acts primarily on slow inactivation of the fast transient $Na^+$ (Errington et al., 2008; Sheets et al., 2008). Future experiments should be aimed at precisely identifying the LCM binding site on $Na^+$ channels, and its overlap with the structures mediating CBZ effects.

Irrespective of the underlying molecular mechanisms, these results show that loss of $\beta_1/\beta_1$B subunits results in loss of CBZ efficacy, whereas this is not the case for the novel anticonvulsant LCM. These data suggest that in disease states associated with loss or modulation of *Scn1b*, LCM may be more efficacious than CBZ in limiting neuronal excitability. However, further data from a relevant disease model or from a clinical study are needed to further establish the clinical utility of LCM in pharmacoresistance potentially arising from loss of $\beta_1$ subunits.

## Acknowledgments

This work was supported by the Deutsche Forschungsgemeinschaft (SFB TR3, Project C7), Nationales Genomforschungsnetzwerk NGFN$^{plus}$ EmiNet, EPICURE, and the BONFOR program of the University of Bonn Medical Center. Supported by UCB Pharma.

## Disclosure

Isabelle Niespodziany and Christian Wolff are employees of UCB Pharma. Heinz Beck and Mischa Uebachs have served as paid consultants of UCB Pharma. The study was supported by UCB Pharma. The remaining authors have no conflict of interest. We confirm that we have read the Journal's position on issues involved in ethical publication and affirm that this report is consistent with those guidelines.

## References

Andurkar SV, Stables JP, Kohn H. (1999) The anticonvulsant activities of N-benzyl 3-methoxypropionamides. *Bioorg Med Chem* 7:2381–2389.

Brandt C, Heile A, Potschka H, Stoehr T, Löscher W. (2006) Effects of the novel antiepileptic drug lacosamide on the development of amygdala kindling in rats. *Epilepsia* 47:1803–1809.

Chen C, Westenbroek RE, Xu X, Edwards CA, Sorenson DR, Chen Y, McEwen DP, O'Malley HA, Bharucha V, Meadows LS, Knudsen GA, Vilaythong A, Noebels JL, Saunders TL, Scheuer T, Shrager P, Catterall WA, Isom LL. (2004) Mice lacking sodium channel beta1 subunits display defects in neuronal excitability sodium channel expression and nodal architecture. *J Neurosci* 24:4030–4042.

Cross SA, Curran MP. (2009) Lacosamide: in partial-onset seizures. *Drugs* 69:449–459.

Duncan GE, Kohn H. (2005) The novel antiepileptic drug lacosamide blocks behavioral and brain metabolic manifestations of seizure activity in the 6 Hz psychomotor seizure model. *Epilepsy Res* 67:81–87.

Ellerkmann RK, Remy S, Chen J, Sochivko D, Elger CE, Urban BW, Becker A, Beck H. (2003) Molecular and functional changes in voltage-dependent $Na^+$ channels following pilocarpine-induced status epilepticus in rat dentate granule cells. *Neuroscience* 119:323–333.

Errington AC, Stöhr T, Heers C, Lees G. (2008) The investigational anticonvulsant lacosamide selectively enhances slow inactivation of voltage-gated sodium channels. *Mol Pharmacol* 73:157–169.

Gastaldi M, Robaglia-Schlupp A, Massacrier A, Planells R, Cau P. (1998) mRNA coding for voltage-gated sodium channel beta2 subunit in rat central nervous system: cellular distribution and changes following kainate-induced seizures. *Neurosci Lett* 249:53–56.

Greenaway C, Ratnaraj N, Sander JW, Patsalos PN. (2011) Saliva and serum lacosamide concentrations in patients with epilepsy. *Epilepsia* 52:258–263.

Kazen-Gillespie KA, Ragsdale DS, D'Andrea MR, Mattei LN, Rogers KE, Isom LL. (2000) Cloning localization and functional expression of sodium channel beta1A subunits. *J Biol Chem* 275:1079–1088.

Kellinghaus C. (2009) Lacosamide as treatment for partial epilepsy: mechanisms of action, pharmacology, effects, and safety. *Ther Clin Risk Manag* 5:757–766.

Kuo CC, Huang RC, Lou BS. (2000) Inhibition of $Na^+$ current by diphenhydramine and other diphenyl compounds: molecular determinants of selective binding to the inactivated channels. *Mol Pharmacol* 57:135–143.

Lees G, Stöhr T, Errington AC. (2006) Stereoselective effects of the novel anticonvulsant lacosamide against 4-AP induced epileptiform activity in rat visual cortex in vitro. *Neuropharmacology* 50:98–110.

Meadows LS, Malhotra J, Loukas A, Thyagarajan V, Kazen-Gillespie KA, Koopman MC, Kriegler S, Isom LL, Ragsdale DS. (2002) Functional and biochemical analysis of a sodium channel beta1 subunit mutation responsible for generalized epilepsy with febrile seizures plus type 1. *J Neurosci* 22:10699–10709.

Müller A, Kukley M, Uebachs M, Beck H, Dietrich D. (2007) Nanodomains of single $Ca^{2+}$ channels contribute to action potential repolarization in cortical neurons. *J Neurosci* 27:483–495.

Nicot A, Ratnakar PV, Ron Y, Chen CC, Elkabes S. (2003) Regulation of gene expression in experimental autoimmune encephalomyelitis indicates early neuronal dysfunction. *Brain* 126:398–412.

Patino GA, Claes LRF, Lopez-Santiago LF, Slat EA, Dondeti RSR, Chen C, O'Malley HA, Gray CBB, Miyazaki H, Nukina N, Oyama F, Jonghe PD, Isom LL. (2009) A functional null mutation of SCN1B in a patient with Dravet syndrome. *J Neurosci* 29:10764–10778.

Ragsdale DS, McPhee JC, Scheuer T, Catterall WA. (1996) Common molecular determinants of local anesthetic antiarrhythmic and anticonvulsant block of voltage-gated $Na^+$ channels. *Proc Natl Acad Sci USA* 93:9270–9275.

Sashihara S, Greer CA, Oh Y, Waxman SG. (1996) Cell-specific differential expression of $Na^+$-channel beta 1-subunit mRNA in the olfactory system during postnatal development and after denervation. *J Neurosci* 16:702–713.

Schaub C, Uebachs M, Beck H. (2007) Diminished response of CA1 neurons to antiepileptic drugs in chronic epilepsy. *Epilepsia* 48:1339–1350.

Sekerli M, Negro CAD, Lee RH, Butera RJ. (2004) Estimating action potential thresholds from neuronal time-series: new metrics and evaluation of methodologies. *IEEE Trans Biomed Eng* 51:1665–1672.

Sheets PL, Heers C, Stoehr T, Cummins TR. (2008) Differential block of sensory neuronal voltage-gated sodium channels by lacosamide [(2R)-2-(acetylamino)-N-benzyl-3-methoxypropanamide] lidocaine and carbamazepine. *J Pharmacol Exp Ther* 326:89–99.

Stöhr T, Kupferberg HJ, Stables JP, Choi D, Harris RH, Kohn H, Walton N, White HS. (2007) Lacosamide a novel anti-convulsant drug shows efficacy with a wide safety margin in rodent models for epilepsy. *Epilepsy Res* 74:147–154.

Sun GC, Werkman TR, Battefeld A, Clare JJ, Wadman WJ. (2007) Carbamazepine and topiramate modulation of transient and persistent sodium currents studied in HEK293 cells expressing $Na_V1.3$ alpha-subunit. *Epilepsia* 48:774–782.

Taverna S, Mantegazza M, Franceschetti S, Avanzini G. (1998) Valproate selectively reduces the persistent fraction of $Na^+$ current in neocortical neurons. *Epilepsy Res* 32:304–308.

Uebachs M, Opitz T, Royeck M, Dickhof G, Horstmann MT, Isom LL, Beck H. (2010) Efficacy loss of the anticonvulsant carbamazepine in mice lacking sodium channel beta subunits via paradoxical effects on persistent sodium currents. *J Neurosci* 30:8489–8501.

Vervaeke K, Hu H, Graham LJ, Storm JF. (2006) Contrasting effects of the persistent $Na^+$ current on neuronal excitability and spike timing. *Neuron* 49:257–270.

Wallace RH, Wang DW, Singh R, Scheffer IE, George A Jr, Phillips HA, Saar K, Reis A, Johnson EW, Sutherland GR, Berkovic SF, Mulley JC. (1998) Febrile seizures and generalized epilepsy associated with a mutation in the $Na^+$-channel beta1 subunit gene SCN1B. *Nat Genet* 19:366–370.

Wang Y, Park KD, Salome C, Wilson SM, Stables JP, Liu R, Khanna R, Kohn H. (2011) Development and characterization of novel derivatives of the antiepileptic drug lacosamide that exhibit far greater enhancement in slow inactivation of voltage-gated sodium channels. *ACS Chem Neurosci* 2:90–106.

Xu J, Kang N, Jiang L, Nedergaard M, Kang J. (2005) Activity-dependent long-term potentiation of intrinsic excitability in hippocampal CA1 pyramidal neurons. *J Neurosci* 25:1750–1760.

Yang YC, Hsieh JY, Kuo CC. (2009) The external pore loop interacts with S6 and S3-S4 linker in domain 4 to assume an essential role in gating control and anticonvulsant action in the $Na^+$ channel. *J Gen Physiol* 134:95–113.

Yue C, Remy S, Su H, Beck H, Yaari Y. (2005) Proximal persistent $Na^+$ channels drive spike afterdepolarizations and associated bursting in adult CA1 pyramidal cells. *J Neurosci* 25:9704–9720.